

Combined EXAFS and XRD for the in situ structural elucidation of solid catalysts under operating conditions

John Meurig Thomas and G. Neville Greaves¹

*Davy Faraday Research Laboratory, Royal Institution of Great Britain,
21 Albemarle Street, London W1X 4BS, UK*

Received 1 March 1993; accepted 6 May 1993

Two distinct kinds of experimental arrangement permit X-ray absorption and X-ray diffraction data to be recorded in a combined manner under in situ conditions. Results are shown for the conversion of a copper–zinc hydroxycarbonate precursor to a “live” water–gas shift catalyst and for a zinc oxide and a zeolite model catalyst heated to ca. 1000°C. The short-range and long-range structural changes accompanying the conversion of the zeolite into cordierite are charted at high temperature. EXAFS and XANES data can be recordable both in fluorescence or transmission mode with one of the arrangements, which also permits successive measurements (around more than one absorption edge) within a short space of time.

Keywords: Quick EXAFS; XRD; XANES; zinc oxide; zeolite; cordierite; copper catalysts

Recently we described [1] how, with a photodiode array for the recording of X-ray absorption signals and a position-sensitive detector for X-ray diffraction, it proved possible to trace changes in both the short-range (up to a radius of 10 Å or so from a central atom) and long-range crystallographic order during the entire course of the production of an active metal catalyst from its compound precursor (fig. 1). Specifically, synthetic variants of the mineral phase aurichalcite ($\text{Cu}_{5-x}\text{Zn}_x(\text{OH})_6(\text{CO}_3)_2$, a layered hydroxycarbonate with Cu/Zn ratios ranging from 0.25 to 1.00) were heated in air up to 450°C to yield mixed oxides of copper and zinc and then reduced so as to produce ZnO-supported metallic copper that could be probed by combined X-ray absorption and X-ray diffraction while functioning as an active catalyst for the water–gas shift reaction ($\text{CO}_2 + \text{H}_2 \rightleftharpoons \text{CO} + \text{H}_2\text{O}$). Although we found there was no evidence for assimilation of Cu(I) species into the ZnO [2], there were nevertheless clear indications of some incorporation of zinc into the metallic copper forming a dilute, disordered phase of brass. Furthermore, in the early stages of the thermal treatment of the

¹ Permanent address: The SERC Daresbury Laboratory, Daresbury, Warrington, Cheshire WA4 4AD, UK.

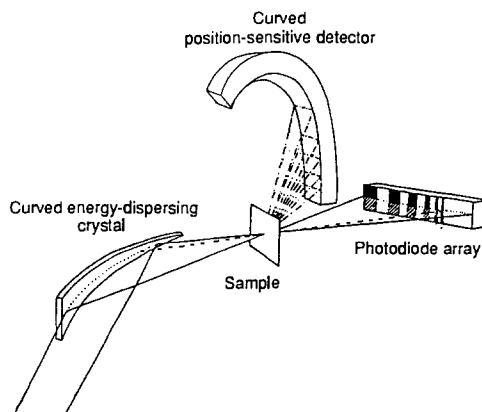


Fig. 1. Fixed-geometry set-up for the combined recording of X-ray absorption spectra (using the photodiode array detector) and X-ray diffraction patterns. The latter are recorded using a curved position-sensitive detector placed vertically above the environmental stage at the focus of the monochromator. (The large handpass required for X-ray absorption spectral measurements results in a slight broadening of the widths of the diffraction peaks – see fig. 2.)

aurichalcite, no significant changes occur (fig. 2) in the local environment of Cu(II) species even though there are drastic changes in crystallinity of the solid precursor as it is heated to drive away water and carbon dioxide and to break down the layered structure of the parent. At ca. 300°C, for example, the solid is essentially X-ray amorphous, yet the local environment of the copper (and zinc) ions remains as it was at room temperature (and stays the same also up to ca. 450°C).

The set-up schematized in fig. 1 has many merits: the fixed geometry arrangement permits the X-ray absorption spectrum and the diffraction pattern of a catalyst to be recorded under actual reaction conditions in very rapid succession (within seconds – and, in principle, on even shorter time scales, provided due attention is paid to the detection systems [3]). But rapidity in recording the X-ray absorption and X-ray diffraction signatures of a solid is not the only (or key) desideratum. In many of the crucial processes occurring within solids during their conversion from inert to active (or “poisoned”) catalysts, or in the processes of catalyst regeneration, the time-scale is frequently much longer, even involving several minutes or hours for one critical phase to be transformed into another. Moreover, there are situations where very high temperature (in excess of 1000°C) may be needed especially when an appropriate catalyst support phase has to be generated. Under these circumstances, the merits of a second method (described below) of recording parallel EXAFS and XRD patterns are considerable.

The schematic arrangement for the recording of “quick” EXAFS (QuEXAFS) combined with XRD patterns of catalysts and catalyst supports is shown in fig. 3. X-ray diffraction (Debye–Scherrer) patterns from such complex catalysts as metal-exchanged zeolites may be routinely obtained in about 400 s with a resolution in

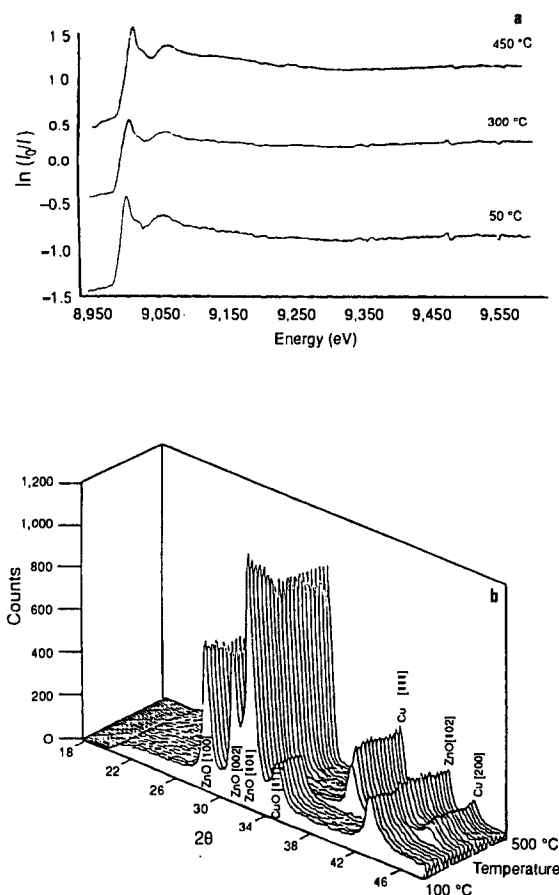


Fig. 2. (a) Raw EXAFS plots above the copper edge, showing that no significant structural changes occur in the immediate vicinity of Cu(II) species in the heated precursor hydroxycarbonate ($\text{Cu}_{5-x}\text{Zn}_x(\text{OH})_6(\text{CO}_3)_2$) even though the corresponding X-ray diffraction patterns (not shown) exhibit major changes over the 50° to 450° range. (b) Temperature-resolved XRD patterns of a 20 : 80 mixture of CuO : ZnO (produced on heating the precursor catalyst in air (see text and (a)) showing changes in composition when the mixture is heated to 500°C in a 10 : 90 H_2 : N_2 gas stream at 2°C m^{-1} . (Note that the (110), (200) and (111) reflections of CuO are observed by the (100), (002) and (101) reflections of ZnO and, for clarity, have not been labelled.)

2-theta of 0.04°. The two-circle monochromator operates by rotating the Bragg angle continuously [4] thereby eliminating, to all intents and purposes, the dead-time associated with conventional angle-by-angle scanning. By using a unique double-encoded dc motor feedback servo system optimised for scanning at constant speed [5] the uncertainties in monochromatic energy calibration associated with stepper motor mechanisms can also be avoided. Speeds of 1 deg s^{-1} are typical with an accuracy of 0.1 mdeg. Combined with the high flux station 9.3 at the Synchrotron Radiation Source [6], EXAFS spectra can be collected either in fluorescence or transmission mode in scan times of between 10 and 300 s i.e. commensurate with

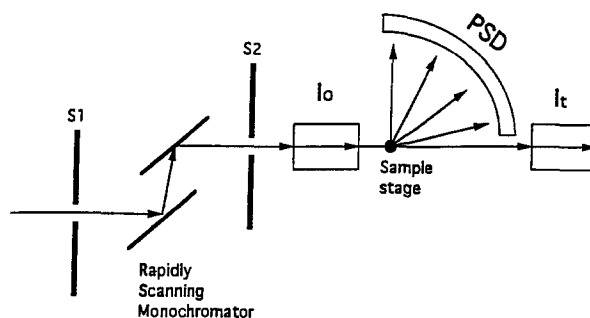


Fig. 3. Schematic diagram of the experimental arrangement used for combined “quick” EXAFS (QuEXAFS) and X-ray diffraction studies of catalysts under operating conditions. Unlike the set-up shown in fig. 1, this arrangement enables EXAFS spectra to be recorded either in fluorescence or transmission mode. S1, entrance slit; S2, exit slit; Io, ion chamber for measuring incident beam; It, ion chamber for measuring transmitted beam; PSD, position sensitive detector (for XRD); sample stage, Linkham environmental cell.

the times required to collect XRD patterns. The rapid slewing rate of the monochromator can also be utilised to ensure that the XRD is measured at a wavelength away from any anomalous region. It can also be used to measure more than one X-ray absorption edge in a short space of time. Whilst QuEXAFS is not as inherently rapid as energy dispersive EXAFS (minutes compared to fractions of a second) it is nevertheless well-suited particularly when it is combined with XRD for charting the changes in structural characterisation associated with a large variety of processes in the chemistry of condensed matter.

We illustrate the power of the QuEXAFS/XRD combined approach by showing preliminary results obtained with an environment cell that permitted a solid state reaction to be studied from room temperature to above 1000°C. This involved the metamorphosis of an ion exchanged zeolite to produce synthetic cordierite ($\text{Mg}_2\text{Al}_4\text{Si}_5\text{O}_{18}$) – a process accelerated by the inclusion of a small quantity (~ 1 wt%) of ZnO. Fig. 4a shows the in situ raw XRD data and fig. 4b the Fourier transform versus distance plots computed from a series of QuEXAFS measurements made above the zinc edge. Dramatic changes occur in the XRD patterns and also in the zinc environment as the temperature is progressively increased. Subtle transformations in the zeolite are at first detected ($< 150^\circ\text{C}$), but these are overtaken when the microporous structure collapses and an amorphous phase is formed around 650°C . The formation of an intermediate crystalline phase can just be detected in the XRD at the point where the ZnO dissolves into the collapsed matrix. The dispersion of zinc into the aluminosilicate structure can be clearly seen in the XAFS Fourier transforms (fig. 4b) where the magnitude of the second peak, which is due to zinc–cation correlations, drops sharply between room temperature and 720°C , signifying the replacement of zinc second neighbours by network forming silicons and aluminiums. Conversion of the amorphous cordierite to

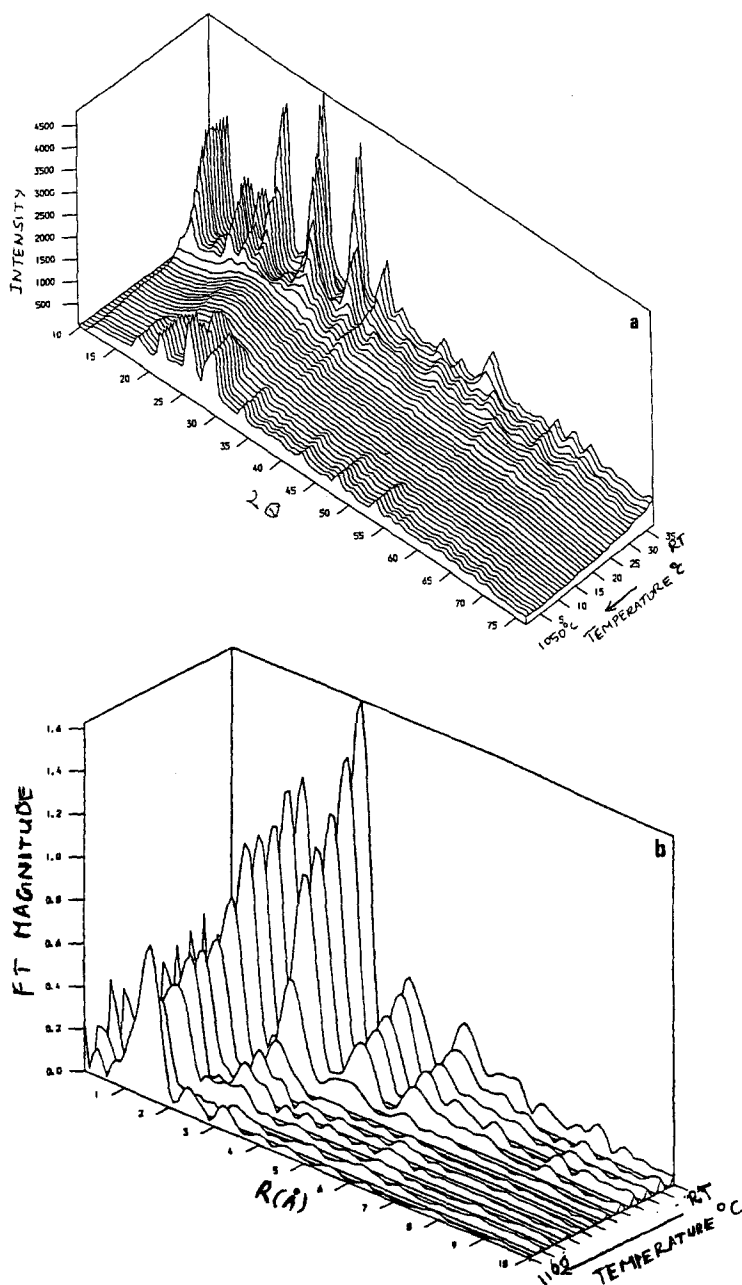


Fig. 4. (a) The raw, in situ X-ray diffraction patterns produced in a temperature-resolved fashion during a thermal excursion of a Mg^{2+} -ion-exchanged zeolite heated with traces of ZnO from room temperature to 1050°C (see text and ref. [7]). The amorphous state formed by the collapse of the zeolite ultimately yields crystalline cordierite. (b) Fourier-transform plots derived from the QuEXAFS data recorded in a temperature-resolved fashion above the zinc edge over a range of temperatures up to 1110°C, under the conditions described in (a) (see text). (Not corrected for phase shift.)

the final mineral phase close to 1000°C is obvious in the powder diffraction and an accompanying modification is recorded in the zinc XAFS, suggesting that zinc enters the crystalline structure.

For completeness we include in fig. 5 a dynamic energy-dispersive (fixed geometry) X-ray diffraction run showing both the peaks and their associated contour representation recorded at 1000°C during the later stages of conversion of the amorphous zeolite to the final crystalline product. This clearly identifies a strong quartz-like (011) line at 30.3 keV prior to the crystallisation of cordierite. From our own studies [7] and from earlier work on the synthesis of cordierite [8,9] this intermediate phase is a stuffed silica having the β -quartz structure. Whilst the overall structures of high quartz and cordierite are totally different, they do share sixfold rings of $(\text{Si}/\text{Al})\text{O}_4$ tetrahedra with Mg^{2+} occupying modifying positions, compensating the AlO_4^- groups [10]. Our findings point to Zn^{2+} infiltrating and straining the β -quartz structure, thereby encouraging a breakdown of the three-dimensional silicate network in favour of the cyclic anion structure of cordierite. Without the inclusion of ZnO the whole process of cordierite crystallisation from the amorphous zeolite is inhibited until much higher temperatures are reached.

The QuEXAFS/XRD combined approach is yielding new insights into the structural chemistry of ceramic formation at high temperatures and the role of dopants. To our knowledge, no other work has reported XAFS measurements

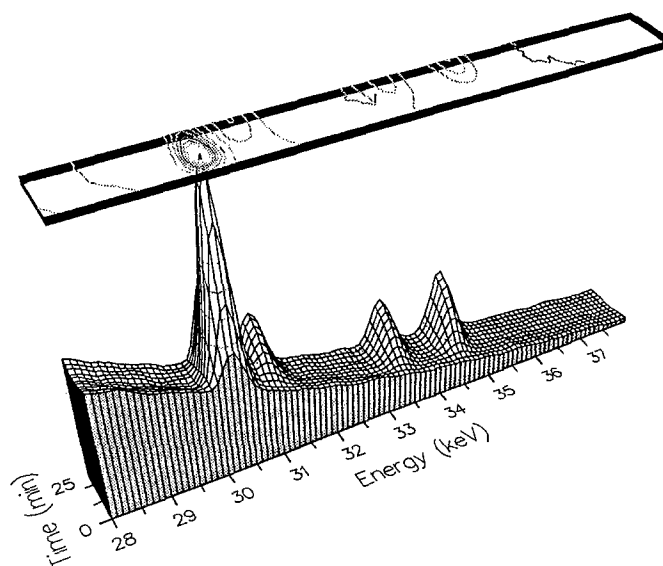


Fig. 5. Energy-dispersive X-ray powder diffraction plots showing the growth and decay of the intermediate stuffed silica phase (30.3 keV line) and the subsequent crystallisation of cordierite as the amorphised zeolite is isothermally treated at 1000°C. The top part shows the contour representation of the peaks.

recorded at such high temperatures; and we are of the opinion that there is a significant improvement in the accuracy of the X-ray data acquirable using the set-up of fig. 3. Further details will be reported elsewhere [7]. With the acknowledged power of XAFS as a tool in the study of solid surfaces and catalysts [7–19] and with the increasingly attractive complementary role of XRD [1,7,18] there are clearly encouraging future prospects for the high temperature studies of operating catalysts.

Acknowledgement

We gratefully acknowledge the support of the Science and Engineering Research Council Laboratory and the experimental assistance of the colleagues mentioned in ref. [7] but especially Dr. G. Sankar.

References

- [1] J.W. Couves, J.M. Thomas, D. Waller, R.H. Jones, A.J. Dent, G.E. Derbyshire and G.N. Greaves, *Nature* 354 (1991).
- [2] L.S. Kau, K.O. Hodgson and E.I. Solomon, *J. Am. Chem. Soc.* 111 (1989) 7103.
- [3] G.E. Derbyshire, D. Bogg, A.J. Dent, R.C. Farrow, G.N. Greaves, W.I. Helsby, C. Morrel, C.R. Ramsdale and M.P. Wells, *Rev. Sci. Instr.* 63 (1992) 790.
- [4] R. Frahm, *Physica B* 158 (1989) 342.
- [5] B.R. Dobson, S.S. Hasnain, M. Neu, C.R. Ramsdale and L.M. Murphy, *Proc. of XAFS VII*, Kobe 1992, in press.
- [6] N. Allinson, G.E. Derbyshire, B.R. Dobson, S. Doyle, G.N. Greaves, N. Harris, P. Mackle, P.M. Moore, J. Nicoll, R.J. Oldman and K.J. Roberts, *Rev. Sci. Instr.* 60 (1989) 1897.
- [7] G. Sankar, G.N. Greaves, J.M. Thomas, A.J. Dent, P.A. Wright, B.R. Dobson, C.R. Ramsdale and S. Natarajan, in preparation.
- [8] W. Schreyer and J.F. Schairer, *Z. Krist.* 116 (1961) 60.
- [9] R.W. Dupon, A.C. Tanous and M.S. Thompson, *Chem. Mater.* 2 (1990) 728.
- [10] R.W.G. Wyckoff, *Crystal Structures* (Wiley, New York, 1968).
- [11] J.H. Sinfelt and G. Meitzner, *Accounts Chem. Res.* 26 (1993) 1.
- [12] H. Kuroda and Y. Iwasawa, *Int. Rev. Phys. Chem.* 10 (1989).
- [13] C.R.A. Catlow and G.N. Greaves, eds., *Applications of Synchrotron Radiation* (Blackie, Glasgow, 1990).
- [14] D.C. Konigsberger et al., in: *10th Int. Congr. on Catalysis*, Budapest, July 1992, Paper 051.
- [15] J.W. Couves, J.M. Thomas, C.R.A. Catlow, G.N. Greaves and A.J. Dent, *J. Phys. Chem.* 94 (1990) 6517.
- [16] M.G. Samant and M. Boudart, *J. Phys. Chem.* 95 (1991) 4070.
- [17] K.R. Kannan, G.U. Kalkarni and C.N.R. Rao, *Catal. Lett.* 14 (1992) 149.
- [18] E. Dooryhee, G.N. Greaves, A.T. Steel, R.P. Townsend, S.W. Carr, J.M. Thomas and C.R.A.C. Catlow, *Faraday Discussions Chem. Soc.* 89 (1990) 119.
- [19] A.T. Ashcroft, A.K. Cheetham, R.H. Jones, S. Natarajan, J.M. Thomas, D. Waller and S.M. Clark, *J. Phys. Chem.* 97 (1993) 3355.